ELSEVIER

Journal of Organometallic Chemistry 562 (1998) 105–114

Journal of Organo metallic Chemistry

New thiophene metallacarbaborane compounds of palladium and platinum: X-ray structures of 1-C_4H_3S-3-(cod)-3,1,2-M-$C_2B_9H_{10}$, 1-C_4H_3S-3,3-$(PMe_2Ph)_2$-3,1,2-Pt–$C_2B_9H_{10}$ and 1-C_4H_3S-3,3-$(PPh_2CH_2CH_2Ph_2)$-3,1,2-Pd-$C_2B_9H_{10}$ (M = Pt or Pd)[1]

Despo M. Michaelidou, D. Michael P. Mingos *, David J. Williams, Andrew W.J. White

Department of Chemistry, Imperial College of Science, Technology and Medicine, South Kensington, London SW7 2AY, UK

Received 22 December 1997

Abstract

The icosahedral metallacarboranes [1-C_4H_3S-3,3-$(PMe_2Ph)_2$-3,1,2-Pt-$C_2B_9H_{10}$], [1-C_4H_3S-3-(cod)-3,1,2-M-$C_2B_9H_{10}$] (M = Pt or Pd) and [1-C_4H_3S-3,3-$(PPh_2CH_2CH_2Ph_2)$-3,1,2-Pd-$C_2B_9H_{10}$] were synthesised from Tl_2[7-(C_4H_3S)-7,8-*nido*-$C_2B_9H_{10}$], [$PtCl_2(PMe_2Ph)_2$], [MCl_2(cod)] (M = Pt or Pd) and [$PdCl_2(PMe_2Ph)_2$], respectively (cod, cyclo-octa-1,5-diene). Their single crystal X-ray structures have been completed and their molecular structures are described. © 1998 Elsevier Science S.A. All rights reserved.

Keywords: Icosahedral metallacarboranes; Platinum carboranes; Polyhedral rearrangements; 'Slip-distortions'

1. Introduction

As part of a study on the effect of substituents on the conformations and skeletal rearrangements of metallacarboranes, a series of thiophene-substituted metallacarboranes of palladium and platinum have been synthesised and structurally characterised. The syntheses and rearrangement properties of phenyl-substituted platinacarbaboranes have been previously reported, for example [1-Ph-3,3-$(PMe_2Ph)_2$-3,1,2,-Pt-$C_2B_9H_{10}$] and the disubstituted compound [1,11-Ph_2-3,3-$(PMe_2Ph)_2$-3,1,11-Pt-$C_2B_9H_9$] [1]. The related palladium compounds [1-Ph-3(cod)-3,1,2-Pd-$C_2B_9H_{10}$] and [Pd(cod)-η^5-7,8-Me_2-7,8-$C_2B_9H_9$] (cod, cyclo-octa-1,5-diene) have been reported by other workers [2,3]. These studies have established that the electronic properties of the metal atom and steric effects associated with substituents on the ligands and the cage both play an important role in influencing the barriers for skeletal rearrangements in these metallacarboranes. The role of steric effects on the conformational preferences and rotational barriers for the rotation of the ML_2 fragments relative to the pentagonal face of the C_2B_9 cage are also of general interest. We recently reported the products of the reaction of $Pd(PMe_2Ph)_2Cl_2$ with Tl_2[7-(RC_4H_2S)-7,8-*nido*-$C_2B_9H_{10}$] (R = Me or H) [4]. This paper discusses the reactions of Tl_2[7-(C_4H_3S)-7,8-*nido*-$C_2B_9H_{10}$] with [$PtCl_2(PMe_2Ph)_2$], [MCl_2(cod)] (M = Pt or Pd) and [$PdCl_2(PMe_2Ph)_2$] and the rearrangement properties of the resulting cage compounds.

2. Experimental details

2.1. Synthesis and characterisation

Reactions were generally performed under N_2 by use of standard Schlenk techniques, although some

---

* Corresponding author. Tel.: +44 171 5945754; fax: +44 171 5945804; e-mail: d.mingos@ic.ac.uk

[1] Dedicated to Prof. R. Bruce King on the occasion of his 65th birthday.

PII S0022-328X(98)00398-2

Table 1
Crystal data, data collection and refinement parameters[a]

Data	**(1)**	**(3)**	**(5)**	**(6)**
Formula	$C_{22}H_{35}B_9P_2SPt$	$C_{14}H_{25}B_9SPt$	$C_{14}H_{25}B_9SPd$	$C_{32}H_{37}B_9P_2SPd$
Solvent	—	—	—	0.5 Me_2CO
Formula weight	685.9	517.8	429.1	748.4
Colour, habit	Deep red blocks	Orange prisms	Red blocks	Orange/brown blocks
Crystal size (mm)	0.43 × 0.27 × 0.27	0.20 × 0.17 × 0.08	0.33 × 0.33 × 0.27	0.56 × 0.47 × 0.17
Lattice type	Monoclinic	Monoclinic	Monoclinic	Triclinic
Space group	$P2_1/c$	Ia[b]	Ia[c]	$P\bar{1}$
Cell dimensions				
a (Å)	14.826(2)	12.458(1)	12.473(1)	10.401(1)
b (Å)	12.662(1)	10.082(1)	10.076(1)	11.076(1)
c (Å)	15.745(2)	15.289(3)	15.335(2)	17.492(3)
α (°)	—	—	—	88.14(1)
β (°)	99.71(1)	98.12(1)	98.76(1)	84.96(1)
γ (°)	—	—	—	74.57(1)
V (Å^3)	2913.3(5)	1901.0(5)	1904.6(3)	1934.8(4)
Z	4	4	4	2
$D_{calc.}$ (g cm^{-3})	1.564	1.809	1.496	1.285
$F(000)$	1344	992	864	764
Radiation used	Mo–K$_\alpha$	Cu–K$_\alpha$	Mo–K$_\alpha$	Mo–K$_\alpha$
μ (mm^{-1})	5.010	14.733	1.077	0.641
θ Range (°)	2.1–25.0	5.3–63.0	2.4–25.0	1.9–25.0
No. of unique reflections				
Measured	5075	1547	1725	6808
Observed [$\lvert F_o\rvert > 4\sigma(\lvert F_o\rvert)$]	3860	1511	1703	5875
Absorption correction	Semi-empirical	Semi-empirical	—	Gaussian
Max, min transmission	0.1677, 0.1033	0.1899, 0.0504	—	0.9079, 0.7483
No. of variables	305	247	247	376
R_1[d]	0.036	0.027	0.022	0.044
wR_2[e]	0.084	0.069	0.058	0.118
Weighting factors a, b[f]	0.040, 4.000	0.069, 0.000	0.035, 0.000	0.066, 1.532
Largest difference peak, hole (e Å^{-3})	0.66, −0.69	0.88, −1.42	0.37, −0.24	0.80, −0.50

[a] Details in common: graphite monochromated radiation, ω-scans, Siemens P4/PC diffractometer, data corrected for Lorentz and polarisation factors, 293 K, refinement based on F^2. [b] I-face centred cell chosen since C-face centred cell has $\beta = 124.2°$. [c] I-face centred cell chosen since C-face centred cell has $\beta = 123.8°$. [d] $R_1 = \Sigma\lVert F_o\rvert - \lvert F_c\rVert/\Sigma\lvert F_o\rvert$. [e] $wR_2 = \sqrt{A}\{\Sigma[w(F_o^2 - F_c^2)^2]/\Sigma[w(F_o^2)^2]\}$. [f] $w^{-1} = \sigma^2(F_o^2) + (aP)^2 + bP$.

subsequent manipulations were carried out in the open laboratory. All solvents were dried and distilled under N_2 prior to use. The NMR spectra were recorded on a JEOL JNM-EX270 FT spectrometer. ^1H, ^{13}C, $^{11}B\{^1H\}$ and $^{31}P\{^1H\}$ chemical shifts (δ) were referenced to tetramethylsilane (^1H, ^{13}C), $BF_3\cdot OEt_2$ and H_3PO_4, respectively. Electron impact (EI) mass spectra were recorded on a VG Micromass 7070B and fast atom bombardment (FAB) mass spectra were recorded on a VG AutoSpecQ mass spectrometer using 3-nitrobenzyl alcohol matrix.

The starting materials [$PdCl_2$(cod)] [5], [$PtCl_2$(cod)] [6] and Tl_2[7-C_4H_3S-*nido*-7,8-$C_2B_9H_{10}$] [4] were made by literature methods.

2.1.1. [1-C_4H_3S-3,3-(PMe_2Ph)$_2$-3,1,2-Pt-$C_2B_9H_{10}$],1

To a mixture of solid Tl_2[7-C_4H_3S-*nido*-7,8-$C_2B_9H_{10}$] (0.605 g, 0.971 mmol) and solid [$PtCl_2$(PMe_2Ph)$_2$] (0.526 g, 0.97 mmol), CH_2Cl_2 (30 ml) was added at −78°C. The reaction mixture was stirred for 1.5 h at intermediate temperatures and 1.5 h at room temperature (r.t.). The resulting orange solution was filtered and the solvent was removed under reduced pressure. Preparative TLC (CH_2Cl_2:hexane, 1:1) gave an intensive orange band ($R_f = 0.21$) as the main product and two very weak bands ($R_f = 0.36$, 0.34). The main product was identified as [1-C_4H_3S-3,3-(PMe_2Ph)$_2$-3,1,2-Pt-$C_2B_9H_{10}$] (**1**) by NMR, MS and a single crystal X-ray analysis. Crystals suitable for X-ray crystallography were grown by layering a CH_2Cl_2 solution with Et_2O at −20°C.

Yield 0.27g, 40%. Anal. Calc. for $C_{22}H_{35}B_9SP_2Pt$; C 38.4, H 5.1%. Found: C 38.4, H 5.1%.

NMR for (**1**): ^1H ($CDCl_3$): δ 7.35 and 7.25 (br s, obscured under $CDCl_3$, 10 H, 2PMe$_2$**Ph**), 7.08 [dd, 1 H, J(H–H) 4.9, J(H–H) 1.3, C_4**H_3**S], 7.03 [dd, 1 H, J(H–

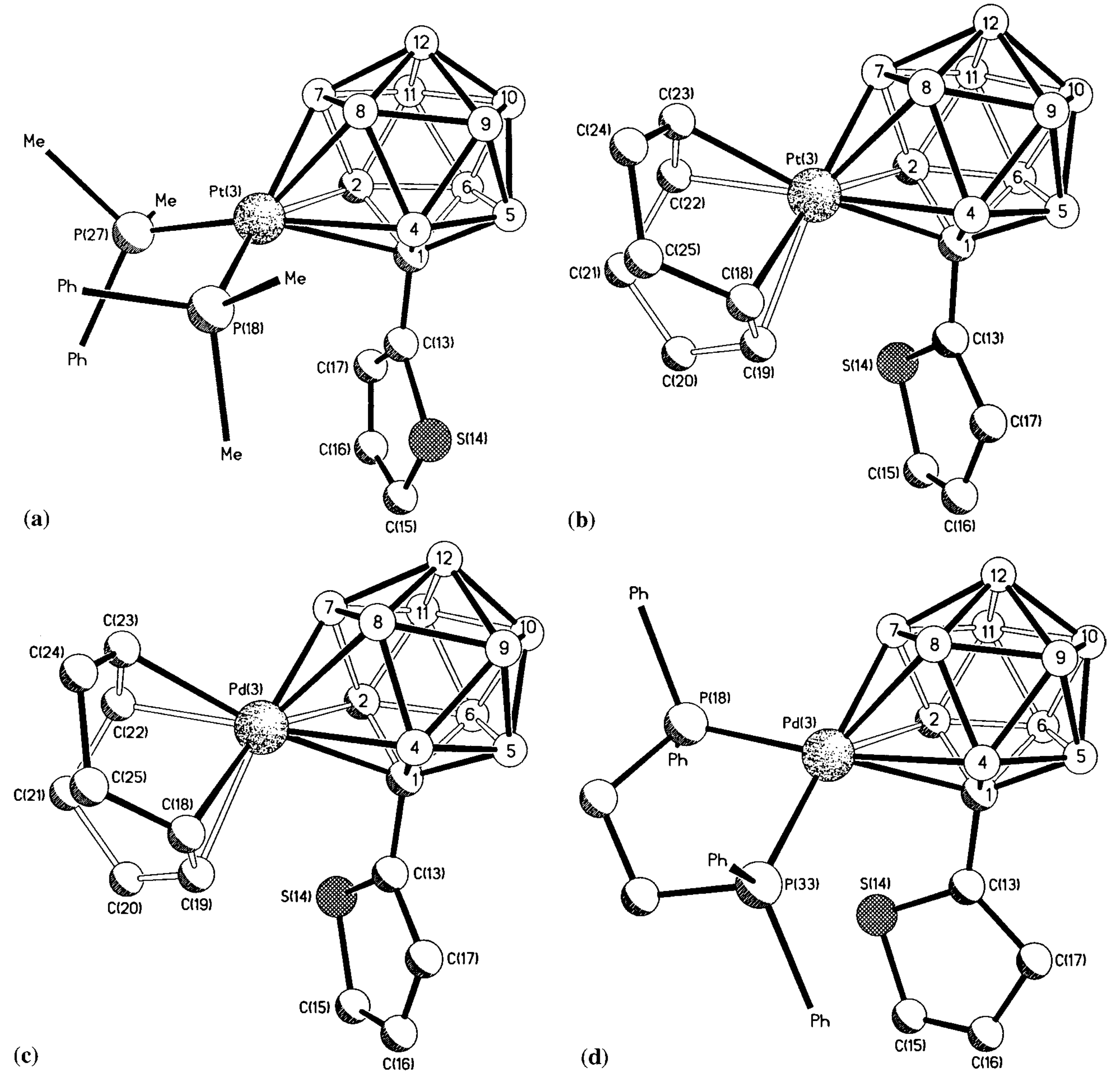

Fig. 1. The molecular structures of **1**, **3**, **5** and **6**—the phenyl rings of the phosphine groups have been omitted for clarity.

H) 3.0, J(H–H) 1.3, $C_4\mathbf{H}_3S$], 6.91 [dd, 1 H, J(H–H) 4.9, J(H–H) 3.6, $C_4\mathbf{H}_3S$], 3.52 (s, 1 H, cage C–**H**), 1.67 (m, 12 H, 2P**Me**$_2$Ph) ppm.

^1H (CD_2Cl_2): δ 7.37 and 7.29 (br s, 10 H, 2PMe$_2$**Ph**), 7.11 [dd, 1 H, J(H–H) 4.9, J(H–H) 1.3, C_4H_3S], 7.03 [dd, 1 H, J(H–H) 3.6, J(H–H) 1.3, $C_4\mathbf{H}_3S$], 6.92 [dd, 1 H, J(H–H) 5.2, J(H–H) 3.6, $C_4\mathbf{H}_3S$], 3.59 (s, 1 H, cage C–**H**), 1.66 (m, 12 H, 2P**Me**$_2$Ph) ppm.

$^{11}B\{^1H\}$ ($CDCl_3$): δ 11.3 (1 B), −4.2 (2 B), −8.9 (1 B), −16.1 (3 B), −19.3 (1 B), −22.0 (1 B) ppm. ^{11}B: doublets $J = 114–127$ Hz.

$^{31}P\{^1H\}$ ($CDCl_3$): δ −10.4 [s, J_1 ($^{31}P–^{195}Pt$) 3362, J_2 ($^{31}P–^{195}Pt$) 3227].

$^{11}B\{^1H\}$ (CD_2Cl_2): δ 11.1 (1 B), −4.5 (2 B), −9.5 (1 B), −15.8 (3 B), −19.5 (1 B), −22.3 (1 B) ppm. ^{11}B: doublets $J = 124–149$ Hz.

Mass spectrum (EI): m/z 686 M^+, 546 M^+ − PMe$_2$Ph, 471 Pt(PMe$_2$Ph)$_2$, 220 $(C_4H_3S)C_2B_9H_{11}$.

2.1.2. [9-C_4H_3S-3,3-$(PMe_2Ph)_2$-3,1,9-Pt-$C_2B_9H_{10}$], 2a and [1-C_4H_3S-3,3-$(PMe_2Ph)_2$-3,1,11-Pt-$C_2B_9H_{10}$], 2b

A sample of compound **1** (30 mg) was dissolved in CD_2Cl_2 in a sealed NMR tube and warmed to 50°C for 3 h. Spectroscopic analysis ($^{31}P\{^1H\}$-, $^{11}B\{^1H\}$-NMR) confirmed the formation of **2a**.

NMR for (**2a**): ^{1}H (CD_2Cl_2): δ 7.2–7.6 (multiplets, 10 H, $2PMe_2\mathbf{Ph}$), 6.93 [dd, 1 H, J(H–H) 5.3, J(H–H) 1.3 $C_4\mathbf{H}_3S$], 7.84 [dd, 1 H, J(H–H) 3.4, J(H–H) 1.5, $C_4\mathbf{H}_3S$], 6.73 [dd, 1 H, J(H–H) 5.3, J(H–H) 3.6, $C_4\mathbf{H}_3S$], 2.73 (s, 1 H, cage C–**H**), 1.68 (br s, 12 H, $2P\mathbf{Me}_2Ph$) ppm.

$^{11}B\{^1H\}$ (CD_2Cl_2): δ − 5.1 (2 B), − 10.1 (2 B), − 16.7 (1 B), − 20.1 (3 B), − 24.4 (1 B) ppm. ^{11}B: doublets $J = 138–159$ Hz.

$^{31}P\{^1H\}$ (CD_2Cl_2): δ − 14.5 [s, $J(^{31}P-^{195}Pt)$ 3327] ppm.

Mass spectrum (EI): m/z 686 M^+, 546 $M^+ -$ PMe_2Ph, 471 $Pt(PMe_2Ph)_2$, 220 $(C_4H_3S)C_2B_9H_{11}$.

A sample of compound **1** was dissolved in toluene and refluxed for 1 h. TLC of the reaction product gave separation of two yellow bands. The second band gave compound **2a**, identified by its ^{11}B-NMR spectrum. The first band allowed isolation of a compound identified as [1-C_4H_3S-3,3-$(PMe_2Ph)_2$-3,1,11-Pt-$C_2B_9H_{10}$] (**2b**) on the basis of the similarity of its ^{11}B-NMR spectrum with that of the structurally characterised compound [1-Ph-3,3-$(PMe_2Ph)_2$-3,1,11-Pt-$C_2B_9H_{10}$] [1].

NMR for (**2b**): $^{11}B\{^1H\}$ (CD_2Cl_2): δ − 8.6 (1 B), − 9.7 (2 B), − 12.2 (1 B), − 13.8 (1 B), − 15.6 (1 B), − 19.1(1 B), − 21.4 (1 B), − 25.5 (1 B) ppm.

2.1.3. [1-C_4H_3S-3-(cod)-3,1,2-Pt-$C_2B_9H_{10}$], 3

To a mixture of solid Tl_2[7-C_4H_3S-*nido*-7,8-$C_2B_9H_{10}$] (0.326 g, 0.52 mmol) and solid [$PtCl_2$(cod)] (0.196 g, 0.52 mmol), CH_2Cl_2 (30 ml) was added at − 180°C. The reaction mixture was allowed to warm to r.t. and was stirred for a further 1.5 h. The resulting brown solution was filtered and the solvent removed under reduced pressure. Preparative TLC (CH_2Cl_2: hexane, 1:1) gave a brown band ($R_f = 0.41$) from which [1-C_4H_3S-3-(cod)-3,1,2-Pt-$C_2B_9H_{10}$] (**3**) was isolated as orange crystals from layering a CH_2Cl_2 solution with pentane. Three more bands were isolated from TLC with $R_f = 0.72$, 0.66 and 0.59.

Table 2
Slip and fold parameters for the metal–carboborane cages in **1**, **3**, **5** and **6**

	1	3	5	6
Δ (Å)[a]	+0.45	+0.34	+0.36	+0.35
θ (°)[b]	3.0	3.6	5.1	4.2
ϕ (°)[c]	4.1	4.6	6.4	5.1
χ (°)[d]	17.8	17.4	16.6	17.9

[a] Calculated as the square root of the difference of the squares of the distance of the metal from the centroid of the lower pentagonal belt and the perpendicular distance of the metal from the plane of this belt. A positive value indicates movement towards B(8) when viewed perpendicular to the plane of the lower pentagonal belt. [b] Calculated as the angle between the plane of the lower pentagonal belt and the C(1)/C(2)/B(4)/B(7) plane. [c] Calculated as the angle between the plane of the lower pentagonal belt and the B(4)/B(7)/B(8) plane. [d] Calculated for the B(8)–H bond with respect to the plane of the lower pentagonal belt, with the hydrogen atoms placed in calculated positions (see Section 2.2).

Yield 0.48 g, 78%. Anal. Calc. for $C_{14}H_{25}B_9SPt$; C 32.5, H 4.83%. Found: C 32.49, H 4.6%.

NMR for (**3**): ^{1}H (CD_2Cl_2): δ 7.05 [dd, 1 H, J(H–H) 5.1, J(H–H) 1.3, $C_4\mathbf{H}_3S$], 6.97 [dd, 1 H, J(H–H) 3.8, J(H–H) 1.3, $C_4\mathbf{H}_3S$], 6.89 [dd, 1 H, J(H–H) 4.9, J(H–H) 3.6 $C_4\mathbf{H}_3S$], 5.60 [m, 2 H, $J(H-^{195}Pt)$ 31.3, =C**H**, cod], 4.65 (m, 2 H, $J(H-^{195}Pt)$ 32.8, =C**H**, cod], 4.57 (s, 1 H, cage C–**H**), 2.66 (m, 4 H, –C$\mathbf{H}_2$, cod), 2.26 (m, 4 H, –C$\mathbf{H}_2$, cod) ppm.

$^{11}B\{^1H\}$ (CD_2Cl_2): δ 10.4 [1 B, $J(^{11}B-^{195}Pt)$ 142], − 3.8 (1 B), − 7.4 (1 B), − 8.8 (2 B), − 11.4 (1 B), − 12.9 (1 B), − 16.1 (br s, 2 B) ppm. ^{11}B: doublets $J = 128–156$ Hz.

$^{13}C\{^1H\}$ (CD_2Cl_2): δ 146.2 (s, **C**, C_4H_3S), 126.8 (s, **C**–H, C_4H_3S), 123.4 (s, **C**–H, C_4H_3S), 123.0 (s, **C**–H, C_4H_3S), 99.9 [s, =**C**H, $J(^{13}C-^{195}Pt)$ 68, cod], 91.9 [s, =**C**H, $J(^{13}C-^{195}Pt)$ 69, cod], 32.6 (s, –**C**H_2, cod), 30.2 (s, –**C**H_2, cod) ppm.

Mass spectrum (EI): m/z 517 M^+, 407 $M^+ -$ cod, 303 $M^+ - (C_4H_3S)C_2B_9H_{10}$.

2.1.4. [9-C_4H_3S-3-(cod)-3,1,9-Pt-$C_2B_9H_{10}$], 4

A sample of compound **3** (30 mg) was dissolved in CD_2Cl_2 in a sealed NMR tube and warmed to 50°C for 15 h. The new NMR spectra were recorded.

NMR: ^{1}H (CD_2Cl_2): δ 7.03 [dd, 1 H, J(H–H) 5.1, J(H–H) 1.3, $C_4\mathbf{H}_3S$], 6.91 [dd, 1 H, J(H–H) 3.7, J(H–H) 1.3, $C_4\mathbf{H}_3S$], 6.77 [dd, 1 H, J(H–H) 5.1, J(H–H) 3.7 $C_4\mathbf{H}_3S$], 5.20–5.45 [m, 4 H, =C**H**, cod], 3.27 (s, 1 H, cage C–**H**), 2.55–3.10 (m, 8 H, –C$\mathbf{H}_2$, cod) ppm.

$^{11}B\{^1H\}$ (CD_2Cl_2): δ − 4.8 (1 B), − 6.6 (2 B), − 9.9 (1 B), − 14.1 (1 B), − 18.9 (1 B), − 20.5 (3 B) ppm.

2.1.5. [1-C_4H_3S-3-(cod)-3,1,2-Pd-$C_2B_9H_{10}$], 5

To a mixture of solid Tl_2[7-(C_4H_3S)-*nido*-7,8-$C_2B_9H_{10}$] (0.433 g, 0.7 mmol) and solid [$PdCl_2$(cod)] (0.196 g, 0.7 mmol), CH_2Cl_2 (30 ml) was added at − 180°C. The reaction mixture was allowed to warm to r.t. and was stirred for a further 2 h. The deep red–black solution formed was filtered from the grey precipitate and the solvent removed under reduced pressure. Preparative TLC (CH_2Cl_2:hexane, 1:1) gave an intense brown band ($R_f = 0.45$) from which [1-C_4H_3S-3-(cod)-3,1,2-Pd-$C_2B_9H_{10}$] was isolated as dark crystals by layering a CH_2Cl_2 solution with Et_2O. Three more bands were isolated from TLC with $R_f = 0.72$, 0.71 and 0.64.

Yield 0.045 g, 15%. Anal. Calc. for $C_{14}H_{25}B_9SPd$; C 39.2, H 5.8%. Found: C 38.5, H 5.7%.

NMR for (**5**): ^{1}H (CD_2Cl_2): δ 7.19 [dd, 1 H, J(H–H) 3.3, J(H–H) 1.3, $C_4\mathbf{H}_3S$], 7.17 [dd, 1 H, J(H–H) 2.1, J(H–H) 1.3, $C_4\mathbf{H}_3S$], 6.96 (dd, 1 H, J(H–H) 4.9, J(H–H) 4.0, $C_4\mathbf{H}_3S$], 5.96 (m, 2 H, =C**H**, cod), 4.97 (m, 2 H, =C**H**, cod), 4.73 (s, 1 H, cage C–**H**), 2.65 (m, 4 H,

Table 3
Selected bond lengths (Å), angles (°) and derived parameters for **1**, **3**, **5** and **6**

	(1) M = Pt	**(3)** M = Pt	**(5)** M = Pd	**(6)** M = Pd
Bond lengths (Å)				
M–C(1)	2.620(6)	2.468(8)	2.521(4)	2.542(4)
M–C(2)	2.445(7)	2.466(8)	2.519(5)	2.516(4)
M–B(4)	2.295(7)	2.259(10)	2.218(5)	2.264(4)
M–B(7)	2.262(8)	2.211(12)	2.186(5)	2.247(4)
M–B(8)	2.227(8)	2.257(15)	2.266(7)	2.273(4)
M–C(18)	—	2.257(9)	2.282(5)	—
M–C(19)	—	2.228(14)	2.247(6)	—
M–C(22)	—	2.218(10)	2.263(5)	—
M–C(23)	—	2.170(11)	2.228(5)	—
M–P	2.250(2) [P(18)], 2.277(2) [P(27)]	—	—	2.261(1) [P(18)], 2.287(1) [P(33)]
C(1)–C(2)	1.533(8)	1.527(10)	1.520(5)	1.524(6)
C(1)–B(4)	1.711(9)	1.822(14)	1.834(7)	1.783(6)
C(2)–B(7)	1.754(10)	1.79(2)	1.777(7)	1.753(7)
B(4)–B(8)	1.860(12)	1.83(2)	1.785(8)	1.785(7)
B(7)–B(8)	1.782(13)	1.86(2)	1.805(8)	1.778(7)
Bond angles (°)				
C(1)–C(2)–B(7)	116.8(6)	111.9(7)	110.8(3)	112.1(3)
C(2)–B(7)–B(8)	104.4(5)	107.5(7)	109.7(3)	108.0(4)
B(4)–B(8)–B(7)	101.9(5)	101.1(8)	99.9(4)	101.7(3)
C(1)–B(4)–B(8)	109.1(5)	107.5(7)	109.2(3)	108.4(3)
C(2)–C(1)–B(4)	106.9(5)	111.2(7)	108.9(3)	108.9(3)
Derived parameters				
A	+0.065 [B(4)][a]	−0.061 [B(8)]	−0.088 [B(8)]	−0.069 [B(8)]
B	0.043	0.042	0.059	0.046
C	−0.044 [B(6)]	−0.066 [B(6)]	−0.084 [B(6)]	−0.061 [B(6)]
D	0.028	0.043	0.054	0.039
E	1.83	1.76	1.79	1.84
F	3.33	3.25	3.29	3.33
G	89	87	87	89

A and **C** are the maximum deviations from planarity (Å) for the upper and lower pentagonal belts, respectively, with a negative value indicating a displacement away from the metal atom. **B** and **D** are the mean deviations from planarity (Å) for the upper and lower pentagonal belts, respectively. **E** and **F** are the perpendicular distances (Å) of the metal atom from the plane of the upper and lower pentagonal belts, respectively. **G** is the angle (°) between the metal coordination plane and the plane of the lower pentagonal belt.

[a] −0.051 for B(8).

$-CH_2$, cod), 2.39 (m, 2 H $-CH_2$, cod), 2.23 (m, 2 H, $-CH_2$, cod) ppm.

$^{11}B\{^1H\}$ (CD_2Cl_2): δ 19.4 (1 B), −1.7 (1 B), −3.6 (1 B), −7.4 (2 B), −8.4 (2 B), −15.0 (1 B), −16.8 (1 B) ppm. ^{11}B: doublets $J = 104–175$ Hz.

$^{13}C\{^1H\}$ (CD_2Cl_2): δ 127.3 (s, **C**–H, C_4H_3S), 124.5 (s, **C**–H, C_4H_3S), 124.0 (s, **C**–H, C_4H_3S), 116.1 (s, =**C**H, cod), 108.4 (s, =**C**H, cod), 30.9 (s, –**C**H_2, cod), 29.0 (s, –**C**H_2, cod) ppm.

Mass spectrum (FAB): m/z 428 M^+.

2.1.6. [1-C_4H_3S-3,3-($PPh_2CH_2CH_2PPh_2$)-3,1,2-Pd-$C_2B_9H_{10}$], 6

To a mixture of dry Tl_2[7-(C_4H_3S)-*nido*-7,8-$C_2B_9H_{10}$] (0.11 g, 0.17 mmol) and dry [$PdCl_2(PPh_2CH_2CH_2PPh_2)$] (0.1 g, 0.17 mmol), THF (30 ml) was added at −78°C. The reaction mixture was allowed to warm to r.t and was stirred for a further 3 h. The resulting deep red solution was filtered. The product was extracted in acetone. TLC in acetone gave a single red band from which the compound [1-C_4H_3S-3,3-($PPh_2CH_2CH_2PPh_2$)-3,1,2-Pd-C_2B_9 H_{10}] (**6**) was isolated.

Yield 0.074 g, 60%. Anal. Calc. for $C_{32}H_{37}B_9P_2SPd \cdot 0.5(CH_3COCH_3)$; C 53.4, H 4.5%. Found: C 53.5%, H 5.2%.

NMR for (**6**): ^1H (CD_3COCD_3): δ 7.92 [m, 4 H, Ph], 7.58 [m, 6 H, Ph], 7.34–7.49 [m, 10 H, Ph], 6.77 [d, 1 H, J(H–H) 5.3, C_4**H**$_3$S], 6.37 [dd, 1 H, J(H–H) 4.9, J(H–H) 3.6, C_4**H**$_3$S], 6.19 [d, 1 H, J(H–H) 3.6, C_4**H**$_3$S], 3.13 [s, 1 H, cage C–**H**], 2.77–2.80 [m, 4 H, **CH**$_2$**CH**$_2$] ppm.

$^{11}B\{^1H\}$ (CD_3COCD_3): δ 16.3 s, −5.4 s, −8.1 s, −11.8 s, −13.6 s, −15.8 s, −19.7 s ppm.

$^{31}P\{^1H\}$ (CD_3COCD_3): δ 55.5 s (ppm).

Mass spectrum (FAB): m/z 719 M^+.

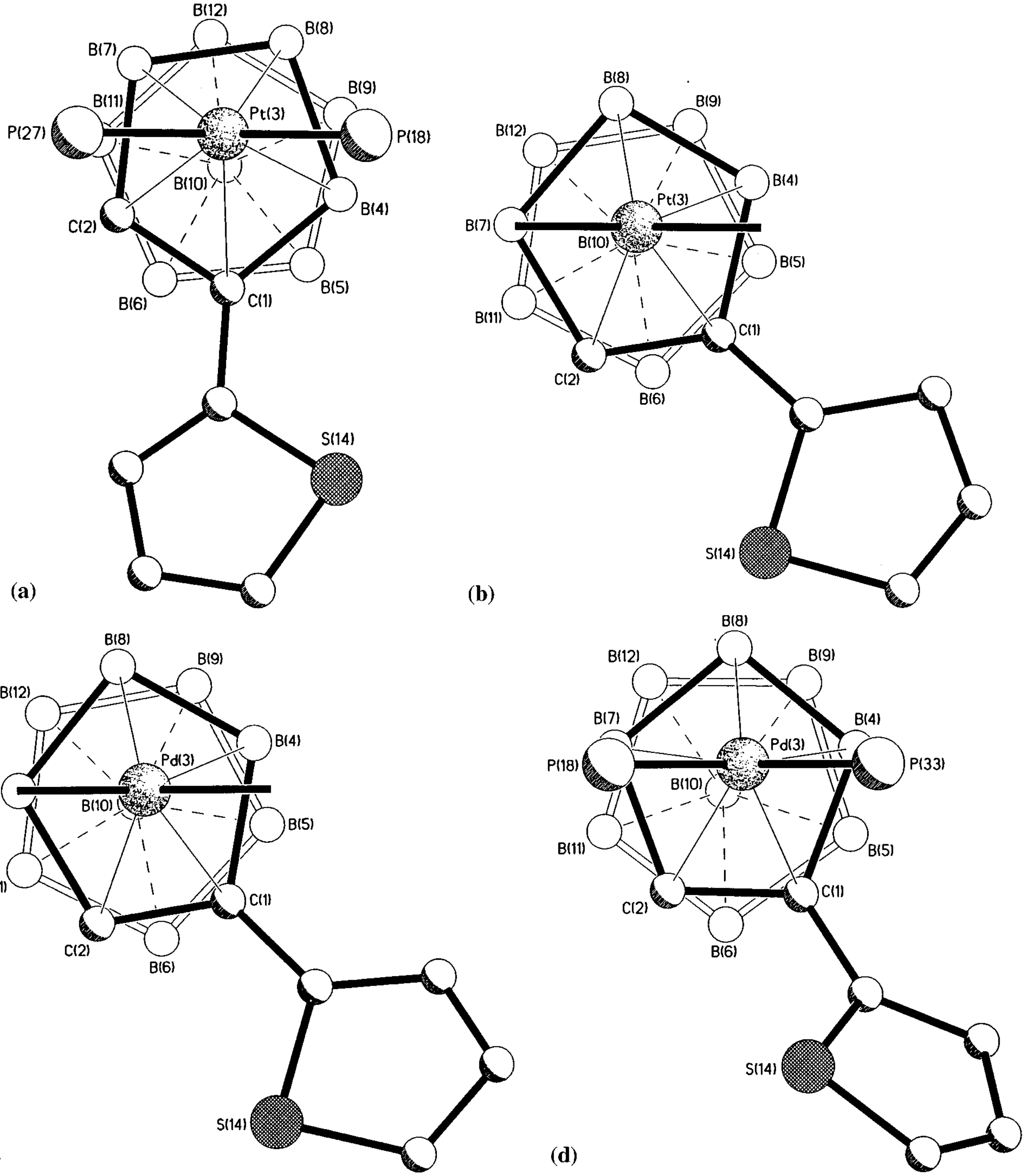

Fig. 2. The structures of **1**, **3**, **5** and **6** viewed in parallel projection in the plane of the coordinated phosphine/cod ligand atoms and down their bisector.

2.1.7. Thermolysis of [1-C_4H_3S-3,3-$(PMe_2Ph)_2$-3,1,2-Pd-$C_2B_9H_{10}$], 7 [4]

A sample of compound **7** (30 mg) was dissolved in CD_2Cl_2 in a sealed NMR tube and warmed to 50°C for 3 h. Spectroscopic analysis ($^{31}P\{^1H\}$-, $^{11}B\{^1H\}$-NMR) showed no change in the original spectra. Some black material was deposited in the NMR tube which indicated partial decomposition.

2.2. Crystallographic studies

A summary of the crystal data, data collection and refinement parameters for **1**, **3**, **5** and **6** is given in Table 1. The platinum structures were solved by the heavy

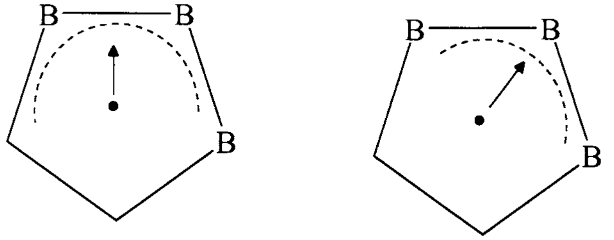

Fig. 3. The possible slip distortions observed in icosahedral metallacarboranes.

atom method and the palladium structures by direct methods. In all four structures, the major occupancy non-hydrogen atoms were refined anisotropically, with the phenyl rings being treated as optimised rigid bodies. In **1**, there is a 75/25 slewing disorder of the phenyl ring in one of the dimethylphenylphosphine ligands. In the isomorphous compounds **3** and **5** there is 65/35 disorder in the orientation of the thiophene ligand, taking, in each case, the form of a ca. 180° rotation about the C(1)–C(13) bond. In **6**, a ΔF map revealed the presence of a 50% occupancy included acetone molecule; this molecule was refined isotropically. In all four structures, the hydrogen atoms were placed in calculated positions, (the B–H hydrogen atoms were placed on the vector representing the negative sum of the five other bonds to the boron atom), assigned isotropic thermal parameters, $U(\mathrm{H}) = 1.2U(\mathrm{eq})$ C–B [$U(\mathrm{H}) = 1.5U(\mathrm{eq})$ C–Me], and allowed to ride on their parent atoms. The polarities of structures **3** and **5** were determined unambiguously by use of the Flack parameter, which refined to values of $-0.02(2)$ and $0.03(4)$, respectively.

For all four structures, the computations were carried out using the SHELXTL PC program system [7]. Additional material available from the Cambridge Crystallographic Data Centre include fractional atomic coordinates, H-atom coordinates, thermal parameters and additional bond lengths and angles.

3. Results

3.1. Synthesis and characterisation

Reaction of $Tl_2[7\text{-}(C_4H_3S)\text{-}\mathit{nido}\text{-}7,8\text{-}C_2B_9H_{10}]$ and *cis*-$[PtCl_2(PMe_2Ph)_2]$ gave the expected icosahedral *closo*-product $[1\text{-}C_4H_3S\text{-}3,3\text{-}(PMe_2Ph)_2\text{-}3,1,2\text{-}Pt\text{-}C_2B_9H_{10}]$, **1**, in 40% yield after purification by TLC. Compound **1** was characterised using NMR, MS and a single crystal X-ray analysis. The $^{31}P\{^1H\}$-NMR spectrum of **1** in $CDCl_3$ at r.t. showed a single resonance at δ -10.4 with a double set of satellites [J_1(P–Pt) 3362, J_2(P–Pt) 3227 Hz] which is consistent with essentially free rotation of the $\{Pt(PMe_2Ph)_2\}$ fragment about the metal–cage axis.

In order to study the skeletal rearrangement behaviour of **1** it was dissolved in CD_2Cl_2 in a sealed NMR tube and the sample was heated to 50°C for 3 h. This caused the original orange colour of the solution to become paler. The $^{31}P\{^1H\}$-NMR spectrum showed the presence of only a single new resonance at δ -14.5 with a single set of Pt satellites J(P–Pt) 3327 Hz. This suggested that **1** was undergoing a specific rearrangement process to quantitatively yield the rearranged product. The rearranged product also formed when a solution of **1** was allowed to stand at r.t. for 10 days. The rearranged product was identified as $[9\text{-}C_4H_3S\text{-}3,3\text{-}(PMe_2Ph)_2\text{-}3,1,9\text{-}Pt\text{-}C_2B_9H_{10}]$, **2a**, by comparing its $^{11}B\{^1H\}$-NMR spectrum with that reported for the

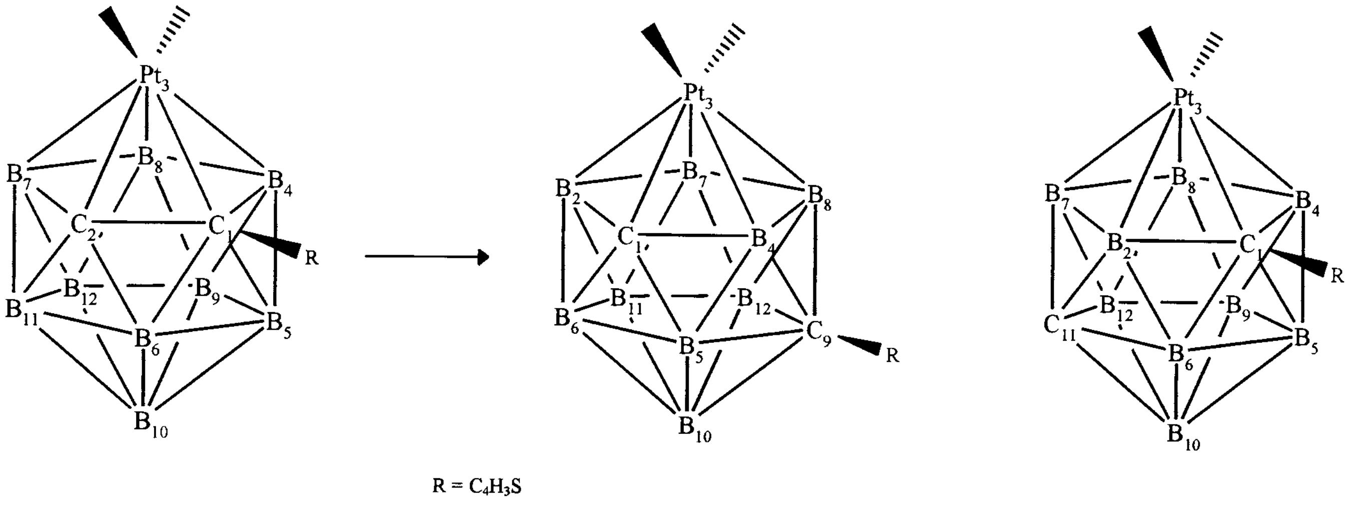

1 **2a** **2b**

Fig. 4. The rearrangement of icosahedral metallacarboranes via a triangular face rotation. (a) This illustrates the effect of an anticlockwise rotation of the C(1)B(5)B(4) face and (b) illustrates a clockwise rotation of the C(2)B(4)B(7) face.

analogous Ph-substituted compound, which has been structurally characterised [1]. Thus **2a** is an isomer of **1** where the {C–C_4H_3S} fragment is located in the lower pentagonal belt with the {CH} fragment in the upper belt. The $^{11}B\{^1H\}$-NMR spectrum of **2a** in CD_2Cl_2 shows five single resonances at δ −5.1 (2 B), −10.1 (2 B), −16.6 (1 B), −20.1 (1 B) and −24.4 (1 B) which reform as doublets in the ^{11}B-NMR spectrum with coupling constants between 138 and 159 Hz. The characteristic and well-separated low field resonance, which is diagnostic of the 3,1,2-Pt–C_2B_9 cage isomer, is absent. Compound **2a** was isolated from the solution and a mass spectrometric analysis showed a molecular ion at 686 and a similar fragmentation pattern to **1**. Heating a toluene solution of **1** gave, after separation by TLC, two yellow bands. The second band corresponded to compound **2a**, whereas the first band gave compound **2b** which was characterised as the rearranged product [1-C_4H_3S-3,3-$(PMe_2Ph)_2$-3,1,11-Pt-$C_2B_9H_{10}$] by comparison of its ^{11}B-NMR spectrum with that of the previously structurally characterised phenyl-substituted analogue [1]. Reaction of [$PtCl_2$(cod)] with the thallium salt Tl_2[7-C_4H_3S-*nido*-7,8-$C_2B_9H_{10}$] gave the expected product **3** as the only isolable product. This reaction resulted in the formation of more complex mixtures of products than that discussed above for the $Pt(PMe_2Ph)_2$ compound. A stationary black band was noted during TLC purification and it was assigned to a decomposition product.

Compound **3** was isolated as orange crystals by layering a CH_2Cl_2 solution with pentane and characterised by NMR spectroscopy and a single crystal X-ray analysis. The $^{11}B\{^1H\}$-NMR spectrum in CD_2Cl_2 showed seven resonances which all showed the expected doublet coupling [$J(B–H) = 128–156$ Hz] in the ^{11}B-NMR spectrum. The low field signal in the $^{11}B\{^1H\}$ spectrum showed an additional set of Pt satellites with $J(^{11}B–^{195}Pt) = 142$ Hz. The $^{13}C\{^1H\}$-NMR spectrum of **3** in CD_2Cl_2 showed three signals at δ 126.8, 123.4 and 123.0 assignable to the CH carbon of the thiophene ring and a singlet at 146.2 assignable to the quaternary C atom. Two singlets at δ 99.9 and 91.9 were observed, assignable to the =CH groups of the cod ligand, both revealing ^{195}Pt satellites with $J(^{13}C–^{195}Pt)$ 68 and 69 Hz, respectively. The two observed singlets at δ 32.6 and 30.2 were finally assigned to the two $-CH_2$ groups of the cod ligand. The observation of only two resonances which may be assigned to cod CH carbons and two to cod CH_2 protons in the ^{13}C-NMR spectrum implies that the cod ligand is free to rotate about the metal axis at ambient temperatures. Compound **1** exhibits similar characteristics. The analogous Pd compound **5** was isolated as the major product from [$PdCl_2$(cod)] with the thallium salt Tl_2[7-C_4H_3S-*nido*-7,8-$C_2B_9H_{10}$], and characterised using NMR, MS and a single crystal X-ray analysis.

Compound **3** was found to rearrange after 15 h heating in a sealed NMR tube. During this time the original spectrum showed the following changes: The thiophene protons moved to 7.03, 6.91 and 6.77 ppm. The peaks at 4.65 (m) and 4.57 (s) disappeared whereas a new broad singlet appeared at 3.27 ppm which was assignable to the new C–H resonance. In the $^{11}B\{^1H\}$-NMR spectrum the peak at 10.4 ppm which is characteristic for a C_2B_3 structure almost disappeared. New resonances appeared at −4.8, −6.6, −9.9, −14.1, −18.9 and −20.5 ppm with an intensity ratio of 1:2:1:1:1:3. This is consistent with a rearrangement process leading to [9-C_4H_3S-3-(cod)-3,1,9-Pt-$C_2B_9H_{10}$] which is analogous to [9-C_4H_3S-3,3-$(PMe_2Ph)_2$-3,1,9-Pt-$C_2B_9H_{10}$] **1**.

Compound **5** was found not to rearrange after prolonged heating in a sealed NMR tube at 55°C. This is consistent with the observation that the Ph analogue does not rearrange [8] but in contrast to the observation by Stone that heating of [Pd(cod)[η^5-7,8-Me_2-$C_2B_9H_9$] results in the formation of the polytopal isomer [Pd(cod)[η^5-2,7-Me_2-$C_2B_9H_9$] [3]. Finally, the reaction of the thallium salt with [$PdCl_2(PPh_2CH_2CH_2Ph_2)$] gave the compound [1-$C_4H_3S$-3,3-$(PPh_2CH_2CH_2PPh_2)$-3,1,2-Pd-$C_2B_9H_{10}$], **6**, as the only product after TLC purification with acetone as eluent. Crystals of **6** were obtained by slow evaporation of an acetone solution and the crystal structure was obtained.

The compound was very sparingly soluble in dichloromethane but soluble enough in acetone for a ^{11}B-NMR spectrum to be obtained.

3.2. Single crystal X-ray analysis discussion

The crystal structures of compounds **1**, **3**, **5** and **6** (shown in Fig. 1a–d) have been determined and a comparative analysis of the 'slip' and 'fold' parameters for the icosahedral carboborane cages in these compounds is presented in Table 2. All of the compounds are based on an icosahedral cage geometry with the two carbons occupying the open pentagonal face. Table 3 gives selected bond lengths and angles for the four structures, together with calculations of the planes for the upper and lower pentagonal belts. The perpendicular distances of the metal atoms from the planes associated with these belts and the inclination of the metal coordination plane to the plane of the lower pentagonal belt are also given. The metal coordination plane is defined as the plane containing the metal and the two phosphorus atoms in the case of **1** and **6**, and the metal atom and the centres of the two double bonds of the cyclooctadiene ligands for the two isomorphous compounds **3** and **5**. The upper and lower pentagonal belts are defined by the atoms C(1)–C(2)–B(7)–B(8)–B(4) and B(5)–B(6)–B(11)–B(12)–B(9), respectively.

In all four structures the plane associated with the lower pentagonal belt of the carbaborane cage is virtually orthogonal to the metal coordination plane. The distance of the metal from the coordinated face of the cage appears to be virtually independent of the nature of the metal atom, but dependent upon the other coordinating ligand(s), with the metal lying closer to this face in the case of the cyclo-octadiene compounds than for those with phosphine based ligands. The metal–phosphine distances are unexceptional and appear to be unaffected by their orientation with respect to the carbaborane cage. The metal–C(carbaborane) distances are fairly similar for all four compounds, though in **1** the Pt–C(1) bond is significantly longer than the corresponding bond in any of the other three structures (vide infra).

The most noticeable differences between the four structures can be appreciated by the views given in Fig. 2a–d. These show each complex viewed from the L_2M direction. In the two cyclooctadiene complexes **3** and **5**, the apical atom of the carboborane cage, B(10), lies only slightly below the horizon of the metal coordination plane, the metal atom in both cases being slipped in the direction of B(9). In the two phosphine complexes **1** and **6** the displacement of B(10) is more marked, the distance below the horizon being in each case very similar, though with the direction of slippage of the metal atom being towards B(12) in **1** but towards B(9) in **6**. The magnitude and variation of these displacements is, however, not apparent from a consideration of the slippage parameter (Δ) in Table 2.

The only other feature of note is the respective orientations of the pendant thiophene ligands with respect to the coordination plane. In **3**, **5** and **6** it is oriented at ca. 5 o'clock whereas in **1** it is positioned at 6 o'clock, a factor that may contribute to the noticeable longer M–C(1) bond in this complex mentioned earlier. The reason for the difference in orientation in the thiophene ligand is not immediately apparent as the steric constraints of the phosphine ligands in **1** and **6** are not that dissimilar. However, the 5 o'clock orientation in **6** is favoured by an intramolecular π-stacking interaction between the thiophene ring and one of the phosphine phenyl rings. The two rings are inclined by only 4° to each other and have a mean interplanar separation of 3.62 Å. An equivalent interaction in **1** is not possible. A discussion of the relative positioning of the sulphur atoms is not pertinent as in two of the structures 180° rotational disorder is observed for these rings.

An inspection of the packing of the molecules in all four structures does not reveal any noteworthy intermolecular packing interactions which could not be considered as resulting from normal van der Waals interactions.

4. Discussion

The structure of compound **1** may be discussed in terms of the bonding between Pt and the C_2B_3 face of the carborane ligand, and whether this bonding predisposes it towards a polyhedral rearrangement process. Kennedy et al. [9] have distinguished two types of bonding in $Pt–C_2B_3$ compounds: a simple ring slippage whereby Pt moves towards the three borons and relatively equally away from the two carbon atoms (their structure type 3B), and an η^4-CB_3 structure, whereby the Pt is located farther from one of the carbons (their structure type 3A) (See Fig. 3).

Kennedy was able to observe both these structures in the unsubstituted compound [3,3-$(PMe_2Ph)_2$-3,1,2-$PtC_2B_9H_{11}$], and points out that therefore steric factors cannot be the underlying cause of the η^4 distorted structures. This had earlier been suggested by Mingos et al. [1], based on structural data on Ph-substituted C(1) carboranes, including an η^4 type structure with Pt–C(1) = 2.596 and Pt–C(2) = 2.362 Å bond lengths. In **1**, the $Pt–C_2B_3$ atom distances also show the molecule to be of the η^4 type, with Pt–C(1) = 2.620 and Pt–C(2) = 2.445 Å.

The rearrangement processes noted for **1** to **2a** and **2b** may be related to rearrangements of similar compounds described previously by ourselves and by Kennedy et al. [9]. The former used microwave dielectric heating to induce the transformation, compared to the thermal or r.t. methods described in this paper. Compounds monosubstituted on C(1) give rearranged products as two isomers. As a result of the rearrangment process the bulky substituent at C(1) or unsubstituted C(2) move out of the C_2B_3 ring to give either a less crowded or more crowded product. In the case of [1-Ph-3,3-$(PMe_2Ph)_2$-3,1,2-$PtC_2B_9H_{10}$], equal amounts of the two isomers were obtained under the vigorous conditions of the microwave experiment [1]. However, in the thermal reaction described here, **1** rearranged to give ca. 80% of the more sterically-favoured (C(1) rearranged) **2a** product and only 20% of the less sterically favoured (C(2) rearranged) **2b** product. Moreover, the r.t. reaction gave **2a** as the only isolated product, thus suggesting that steric interactions do indeed contribute significantly to the activation energies for the rearrangement process in these systems.

In general, the rearrangement of icosahedral carboranes and metallacarboranes (Fig. 4) where the C(1)–C(2) connectivity is broken has been discussed in terms of a diamond–square–diamond (DSD) mechanism. However, as Bruce King elegantly demonstrated [10] it is not possible to isomerise icosahedral boranes, carboranes or metallacorborane via a single DSD process—multiple DSD's are required. The products of the rearrangement of **1** to form **2a** and **2b** may be accounted for in terms of a triangular face rotation. Thus for the formation of **2a**, the triangular face C(1)–B(5)–B(6) of **1** rotates by 60° clockwise so that C(1) moves to the position of B(5), B(5) to that of B(6) and B(6) to that of C(1) (Fig. 4). Similarly, for the formation of **2b** the triangular face C(2)–B(11)–B(6) in **1** rotates by 60° anticlockwise so that C(2) moves to the position of B(11), B(11) to B(6), and B(6) to C(2). However, this does not mean that the mechanism actually involves a triangular face rotation. A recent paper by Welch and Weller [11] has shown that for a sterically crowded molybdenum carborane it is possible to isolate an intermediate for the rearrangement process, which results from multiple DSD processes and has two four and two six connected vertices. This molecule rearranges on heating to give an icosahedral isomer analogous to that described above. Thus isomerisation of a 3,1,2-MC_2B_9 architecture is a complex process which probably involves several DSD processes and may also require the formation of an alternative poyhedral entity as an intermediate.

The experiments we have described have shown that the platinum compounds rearrange more readily than the palladium compounds. This illustrates how the nature of the metal atom can greatly influence the ease with which carbametalloboranes undergo polyhedral rearrangement. This observation is in agreement with Stone et al. who have previously demonstrated the greater tendency of the third row transition metal (W) carbametalloboranes to undergo rearrangement compared to their second row (Mo) analogues in chemical reactions [12,13].

Acknowledgements

We would like to thank BP for endowing D.M.P. Mingos's Chair and the EPSRC for financial support to D.M. Michaelidou.

References

[1] (a) D.R. Baghurst, R.C.B. Copley, H. Fleisher, et al., J. Organomet. Chem. 447 (1993) C14–C17. (b) D.R. Baghurst, Ph.D. Thesis, Oxford University, 1992.

[2] G.O. Kyd, L.J. Yellowlees, A.J. Welch, J. Chem. Soc. Dalton Trans. (1994) 3129.

[3] K.A. Fallis, D.F. Mullica, E.L. Sappenfield, F.G.A. Stone, Inorg. Chem. 33 (1994) 4927.

[4] D.M. Michaelidou, D.M.P. Mingos, D.J.W. Williams, A.W.J. White, J. Organomet. Chem. 528 (1997) 135.

[5] D. Drew, J.R. Doyle, Inorg. Synth. 13 (1972) 52.

[6] H.C. Clark, L.E. Manzer, J. Organomet.Chem. 59 (1973) 411.

[7] SHELXTL PC version 5.03, Siemens Analytical X-Ray Instruments, Madison, WI, 1994.

[8] T.D. McGrath, A.J Welch, J. Chem. Soc. Dalton Trans. (1995) 1755.

[9] D. O'Connell, J.C. Patterson, T.R. Spalding, et al., J. Chem. Soc. Dalton Trans. (1996) 3323.

[10] R.B. King, Inorg. Chim. Acta 49 (1981) 237.

[11] S. Dunn, G.M. Rosair, R.L. Thomas, A.S. Weller, A.J. Welch, Angew. Chem. Int. Ed. Engl. (1997) 645.

[12] S.A. Brew, N. Carr, J.C. Jeffrey, M.U. Pilotti, F.G.A. Stone, J Am. Chem. Soc. 114 (1992) 2203.

[13] S. Li, F.G.A. Stone, Polyhedron 12 (1993) 1689.